Journal of Nuclear Materials 397 (2010) 132–134

Contents lists available at ScienceDirect

Journal of Nuclear Materials

journal homepage: www.elsevier.com/locate/jnucmat

Letter to the Editor

Strain-induced drift of interstitial atoms in SiC implanted with helium ions at elevated temperature

S. Leclerc [a,b], M.F. Beaufort [a], A. Declémy [a], J.F. Barbot [a,*]

[a] *Laboratoire de Physique des Matériaux, UMR6630-CNRS, Université de Poitiers, Boulevard M. et P. Curie, SP2MI, BP 30179, 86962 Futuroscope, France*
[b] *CEMHTI-CNRS, 3A rue de la Férollerie, 45071 Orléans Cedex 2, France*

ARTICLE INFO

Article history:
Received 9 September 2009
Accepted 17 December 2009

ABSTRACT

The effects of temperature on helium implanted SiC were investigated through X-ray diffraction measurements. At low fluence and elevated temperature, dynamic annealing occurs resulting from point defect recombination. At high fluence, the dynamic annealing taking place in the near surface region is concomitant with the formation of a thin and deep highly strained region resulting from the accumulation of interstitial atoms drifted to the deep damaged region under the actions of strain gradient and temperature.

© 2009 Elsevier B.V. All rights reserved.

1. Introduction

SiC is a ceramic with properties making it a good candidate for working in hostile environment and in nuclear and space-based equipment. In particular, because of a low cross-section for neutron capture, it exhibits a low induced activity from exposure in neutron irradiation environments. As a result, SiC has been proposed for structural components in nuclear fusion reactors and as encapsulating material for nuclear fuel in light water reactors and gas-cooled fission reactors [1,2]. A better understanding of the behavior of SiC under irradiation is thus of crucial importance. In the nuclear reactor environment, SiC would be subjected to high fluxes of fast neutrons inducing high levels of atomic displacements and would also develop a high concentration of noble gases, among which helium, produced by nuclear reactions. The nuclear use of SiC would also imply that radiation damage forms at high temperature where a competition between recombination and agglomeration of point defects is likely to take place. A significant simultaneous defect recombination has already been observed at temperatures as low as 300 K [3]. The formation at high implantation temperatures of complex defects that are more difficult to anneal out than those produced at room temperature has also been shown to occur [4,5]. In SiC, amorphization is known to result from the dynamical competition between damage production and recovery during irradiation, and occurs only below a critical temperature decreasing with particle mass [6]. Beyond this temperature, the saturation of the concentration of the implantation-induced-defects has been reported in the near surface region, i.e., where the nuclear energy losses are low [7]. Yet, studies are required to understand the processes taking place while performing implantations at elevated temperature in SiC. In the present work, the combined effects of temperature and fluence of helium implantation were studied through the measurement of the implantation-induced strain by X-ray diffraction (XRD).

2. Experimental

The samples used in this study were n-type $(0\,0\,0\,1)_{Si}$ 4H–SiC single crystals (grown 8° off-axis towards the $[1\,1\,\bar{2}\,0]$ direction) of resistivity 0.02 Ω cm supplied by Cree Research Incorporation. Two sets of ^{4}He ion implantations were carried out at chosen fluences of 1×10^{16} and 5×10^{16} cm^{-2} for a given incident energy of 160 keV. According to TRIM 2003 [8], the distribution of 160 keV helium ions peaks at $R_p \approx 590$ nm with a straggling of about 80 nm. The damage reaches 0.15 dpa and 0.75 dpa at low and high fluence, respectively, assuming displacement energies of 20 eV for the C sublattice and 35 eV for the Si sublattice. Each set consists of implantations at 30 °C, 200 °C, 500 °C and 800 °C. Additional ^{3}He implantations at fluences giving equivalent damage peaks in displacement per atom were performed to determine the helium profiles by using nuclear reaction analysis (NRA) experiments. A low beam-current density of about 4 μA cm^{-2} was used to prevent any additional beam heating during implantation. Previous studies have shown that ion implantation induces a strain gradient in the direction normal to the sample surface [7,9,10]. The strain gradient was studied through XRD measurements conducted on an automated laboratory-made two-circle goniometer with the radiation (λ = 1.5405 Å) provided by a 5 kW RIGAKU RU-200 generator with a vertical linear focus in combination with a quartz

* Tel.: +33 5 49 49 67 34; fax: +33 5 49 49 66 92.
E-mail address: jean.francois.barbot@univ-poitiers.fr (J.F. Barbot).

0022-3115/$ - see front matter © 2009 Elsevier B.V. All rights reserved.
doi:10.1016/j.jnucmat.2009.12.011

monochromator. The two-circle goniometer enables the independent rotations of the sample (ω) and the detector (2θ) around the same axis. In addition, the sample holder can rotate around and translate along two other perpendicular axes enabling the fine alignment of monocrystalline samples. Near surface and maximum strains, $(\Delta d/d)_S$ and $(\Delta d/d)_M$, were obtained from experimental $\omega - 2\theta$ scans performed along the surface normal direction. The scans were then manually fitted using a web-based program written by Stepanov [11] to obtain the strain profiles as a function of depth from the experimental varying interference fringe period. The program implements a "discrete" algorithm; the damaged layer of crystal is divided by the user onto sublayers of given parameters among which thickness and normal strain. This strain profile is progressively modified by the experimenter until the calculated XRD curve fits the experimental one. Although high accuracy is obtained on the width of the strain profiles, the exact position of the strain profiles with respect to the sample surface cannot be accurately determined from such X-ray data. As the normal strain partly results from the defects generated by implantation, the strain profiles were centered on the position of the peak in the TRIM nuclear energy loss distribution in agreement with previous Large Angle Convergent Beam Electron Diffraction experiments [12]. More information on the XRD set-up, experimental and simulation procedures are displayed elsewhere [7].

3. Results and discussion

In Fig. 1 are plotted the XRD curves of the samples implanted with He ions to the fixed fluences of (a) 1×10^{16} cm^{-2} (0.15 dpa at the damage peak) and (b) 5×10^{16} cm^{-2} (0.75 dpa at the damage peak) at different temperatures. Whatever the temperature of implantation and for both fluences, the curves show a tail of scattered intensity toward the low angle side of the Bragg peak ($-(\Delta d/d)_N = 0$) that is characteristic of a dilatation gradient of the lattice along the direction perpendicular to the sample surface. Except for the sample implanted at RT to 5×10^{16} cm^{-2}, the scattered intensity consists of an asymmetrical satellite peak close to the Bragg peak followed by an interference fringe pattern. The satellite peak results from the diffraction of the near surface region while the fringes result from the coherent diffraction of two damaged zones of a same level of strain on either sides of R_p [7]. When performing implantation at RT to 5×10^{16} cm^{-2}, a continuous buried amorphous layer, 180 nm thick, forms in the region of maximum damage as observed by transmission electron microscopy (TEM). The crystalline zones on either sides of the amorphous layer diffract incoherently and the resulting scattered intensity decreases monotonically from the near surface satellite peak down to the background level impeding the determination of the maximum strain.

The values of strain in the near surface region and in the highly damaged region, respectively given by the positions of the satellite peak and of the last fringe away from the Bragg peak, are listed in Table 1 as a function of implantation conditions. At low fluence, 1×10^{16} cm^{-2}, both the near surface and maximum strains decrease with increasing implantation temperature clearly showing the enhancement of dynamic annealing with increasing temperature. In particular, a strong enhancement of the dynamic annealing occurs for temperatures lower than 200 °C, in agreement with previous studies [13,14]. In addition, the ratio maximum strain/near surface strain, $(\Delta d/d)_{M/S}$, decreases with increasing temperature showing that the recovery rate increases with the nuclear energy losses, i.e., with the defect density.

The evolution with implantation temperature of the near surface strain of samples implanted at both fluences is plotted in Fig. 2. Both curves follow the same trend: a decrease with increasing temperature of implantation. The decrease is more pronounced at high fluence which confirms the enhancement of dynamic annealing with defect density.

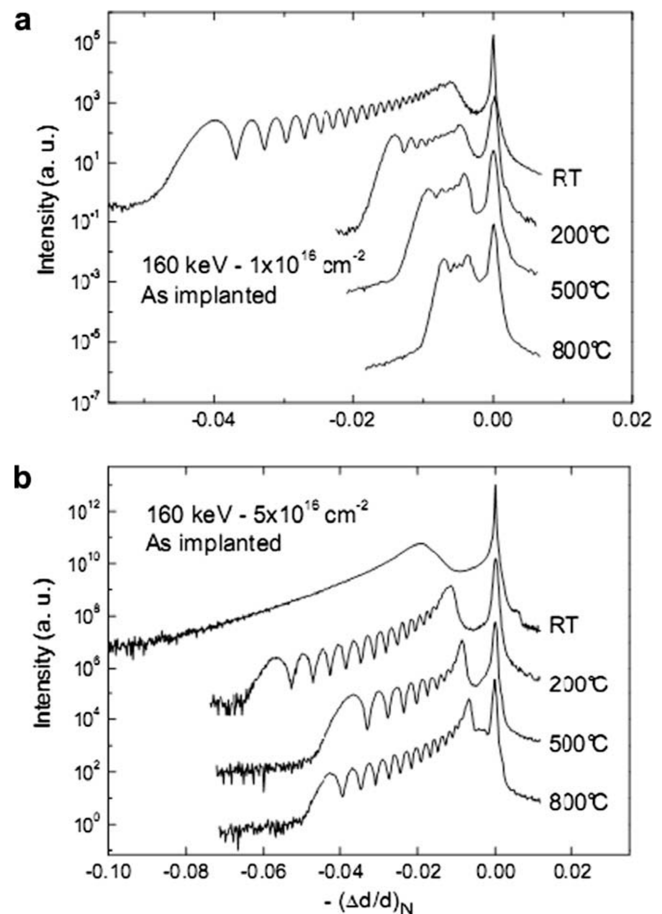

Fig. 1. Experimental $\omega - 2\theta$ scans performed along the surface normal direction close to the (0 0 0 4) reflection in He-implanted 4H–SiC (160 keV) at different implantation temperatures to a fixed fluence of (a) 1×10^{16} cm^{-2} (0.15 dpa at damage peak) and (b) 5×10^{16} cm^{-2} (0.75 dpa at damage peak). The X-ray scattered intensity is plotted as a function of the normal strain $(\Delta d/d)_N$ obtained from the deviation to the Bragg angle [7].

Table 1
Near surface strain and maximum strain values, respectively noted $(\Delta d/d)_S$ and $(\Delta d/d)_M$, as a function of he implantation conditions (160 keV). The ratio between the maximum strain value and the near surface strain value, $(\Delta d/d)_{M/S}$, is also reported.

Fluence (cm^{-2})	1×10^{16}				5×10^{16}			
Temperature (°C)	30	200	500	800	30	200	500	800
$(\Delta d/d)_S$ (%)	0.60	0.47	0.41	0.38	1.9	1.2	0.85	0.67
$(\Delta d/d)_M$ (%)	4.3	1.5	1.0	0.8	>9	5.9	4.0	4.5
$(\Delta d/d)_{M/S}$	7.17	3.19	2.44	2.11		4.92	4.71	6.72

It thus appears that the strain could be easily anticipated and controlled through the fluence (dpa) and the temperature of implantation. There is, however, a certain stage where the strain does not seem to be predictable: in the highly damaged region of samples implanted in the high fluence regime. In this case, the results do not follow the tendencies previously described. In particular, the value of maximum strain obtained at 5×10^{16} cm^{-2} after He implantation at 800 °C is unexpectedly higher than the one obtained at 500 °C (see Table 1). This particular behavior is indicative of another mechanism occurring in the highly damaged region of samples implanted at high fluence and elevated temperatures. This is obvious when comparing the strain profiles obtained

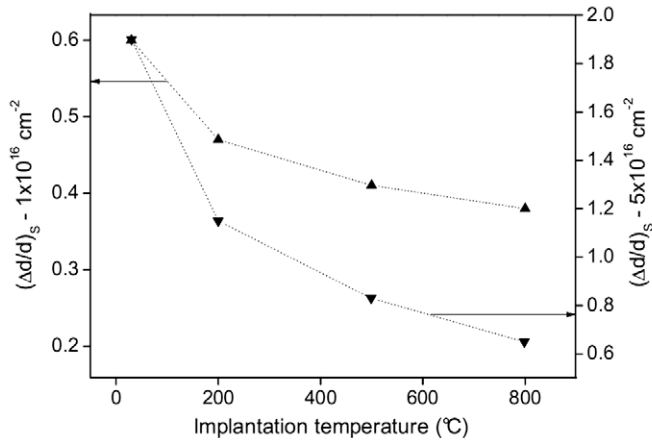

Fig. 2. Comparison of the evolution with implantation temperature of the near surface strains in 4H–SiC implanted with He ions at 160 keV–1×10^{16} and 5×10^{16} cm^{-2} (proportional scales).

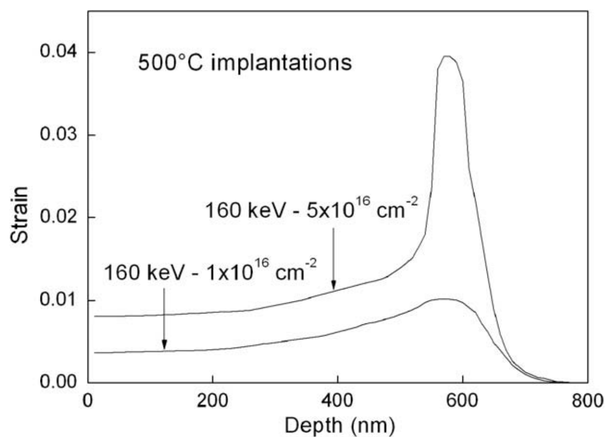

Fig. 3. Strain profiles obtained after He implantations at a fixed temperature of 500 °C to fluences of 1×10^{16} cm^{-2} and 5×10^{16} cm^{-2} (160 keV).

for both fluences at a fixed temperature (see Fig. 3). While the variation of strain is smooth on the entire damaged region of the 1×10^{16} cm^{-2} implanted sample, an abrupt variation of strain occurs in the highly damaged region of the sample implanted at 5×10^{16} cm^{-2}. In this buried region, over about 100 nm, the strain is strongly magnified compared to the maximum strain at lower fluence. For the three studied elevated temperatures, the FWHM of the strain profile at 5×10^{16} cm^{-2} (~80 nm) is lower than both the FWHM of the theoretical nuclear energy loss (~220 nm) and helium concentration profiles (~140 nm). This is contrary to what is reported for room temperature implantations [15] where the strain profiles follow either the TRIM calculated profiles of the nuclear energy losses or the implanted helium depending on the helium concentration. This feature clearly shows that the strain magnification is related to species that migrate toward a thin highly damaged region. The results of NRA depth profiling show that the helium profiles are identical whether the implantation is performed at room temperature or elevated temperature, and at 0.15 or 0.75 dpa at the damage peak. The species involved in the strong positive volume changes in a deep region of samples implanted at elevated temperature and fluence are therefore unambiguously related to defects and mainly to interstitial-type defects. Indeed, most of the defects are supposed to cause the cell to expand; however, theoretical calculations have shown that interstitials induce the largest expansion [16]. The interstitials created during implantation in the near surface region are driven toward the deep highly damaged region under the combined effects of temperature and strain gradient. The migration of interstitial-type defects to the highly strained region together with the recombination of point defects, both enhanced by the fluence, results in the formation of an extended near surface region where scarcely any variation of strain is observed. This leads to the saturation of the near surface strain beyond a threshold fluence as previously observed in SiC implanted with He ions at 600 °C [7].

4. Summary

The sensitivity of XRD strain measurements to point defects, and more particularly to interstitials, has enabled the distinction as a function of fluence of two stages of damage production in SiC implanted with helium ions at elevated temperatures. At low fluence, a dynamic annealing increasing with the defect density has been seen to occur in the whole implanted zone. Accordingly, it has been ascribed to the recombination of point defects. At high fluence, another mechanism takes place. In the extended near surface region, both the recombination of point defects and the migration of interstitial-type defects enhanced by the temperature and the strain gradient, result in a nearly constant strain that levels off at sufficient fluence. Deeper in the sample, in a very narrow region, a strain magnification occurs resulting from the accumulation of interstitial-type defects supplied by the near surface region.

Acknowledgment

T. Sauvage for NRA experiments performed with the 3 MV Van de Graaff accelerator at the CEMHTI Orléans.

References

[1] B.G. Kim, Y. Choi, J.W. Lee, Y.W. Lee, D.S. Sohn, G.M. Kim, J. Nucl. Mater. 281 (2000) 163.
[2] E.E. Bloom, J.T. Busby, C.E. Duty, P.J. Maziasz, T.E. McGreevy, B.E. Nelson, B.A. Pint, P.F. Tortorelli, S.J. Zinkle, J. Nucl. Mater. 367–370 (2007) 1.
[3] W. Jiang, W.J. Weber, S. Thevuthasan, D.E. McCready, J. Nucl. Mater. 257 (1998) 295.
[4] E. Wendler, A. Heft, W. Wesch, Nucl. Instrum Methods Phys. Res. B 141 (1998) 105.
[5] C.H. Zhang, S.E. Donnelly, V.M. Visknyakov, J.H. Evans, J. Appl. Phys. 94 (2003) 6017.
[6] W.J. Weber, Nucl. Instrum Methods Phys. Res. B 166-167 (2000) 98.
[7] S. Leclerc, A. Declémy, M.F. Beaufort, C. Tromas, J.F. Barbot, J. Appl. Phys. 98 (2005) 113506.
[8] J.F. Ziegler, J.P. Biersack, U. Littmark, The Stopping and Range of Ions in Solids, <http://www.srim.org>.
[9] S.I. Rao, C.R. Houska, J. Mater. Sci. 25 (1990) 2822.
[10] G. Bai, M.-A. Nicolet, J. Appl. Phys. 70 (1991) 649.
[11] S. Stepanov, GID-sl. <http://sergey.gmca.aps.anl.gov/gid_sl.html>.
[12] M.F. Beaufort, F. Pailloux, A. Declémy, J.F. Barbot, J. Appl. Phys. 98 (2003) 7116.
[13] A. Hallen, P.O. Persson, A. Yu Kuznestsov, L. Hulman, B.G. Svensson, Mater. Sci. Forum. 338–342 (2000) 849.
[14] R. Héliou, J.L. Brebner, S. Roorda, Semicond. Sci. Technol. 16 (2001) 836.
[15] S. Leclerc, M.F. Beaufort, A. Declémy, J.F. Barbot, Appl. Phys. Lett. 93 (2008) 122101.
[16] J. Li, L. Porter, S. Yip, J. Nucl. Mater. 255 (1998) 139.